

Determining the interaction behavior of calf thymus DNA with berberine hydrochloride in the presence of linker histone: a biophysical study

Louisa Roudini, Negar NayebZadeh Eidgahi, Hamid Reza Rahimi, Mohammad Reza Saberi, Zeinab Amiri Tehranizadeh, Sima Beigoli & Jamshidkhan Chamani

To cite this article: Louisa Roudini, Negar NayebZadeh Eidgahi, Hamid Reza Rahimi, Mohammad Reza Saberi, Zeinab Amiri Tehranizadeh, Sima Beigoli & Jamshidkhan Chamani (2019): Determining the interaction behavior of calf thymus DNA with berberine hydrochloride in the presence of linker histone: a biophysical study, Journal of Biomolecular Structure and Dynamics, DOI: [10.1080/07391102.2019.1574240](https://doi.org/10.1080/07391102.2019.1574240)

To link to this article: <https://doi.org/10.1080/07391102.2019.1574240>



Published online: 17 Feb 2019.



Submit your article to this journal [↗](#)



View Crossmark data [↗](#)



Determining the interaction behavior of calf thymus DNA with berberine hydrochloride in the presence of linker histone: a biophysical study

Louisa Roudini^a, Negar NayebZadeh Eidgahi^a, Hamid Reza Rahimi^{b,c}, Mohammad Reza Saberi^d, Zeinab Amiri Tehranizadeh^d, Sima Beigoli^e and Jamshidkhan Chamani^a

^aDepartment of Biology, Faculty of Sciences, Mashhad Branch, Islamic Azad University, Mashhad, Iran; ^bNeurogenic Inflammation Research Center, Mashhad University of Medical Sciences, Mashhad, Iran; ^cDepartment of Modern Sciences & Technologies, School of Medicine, Mashhad University of Medical Sciences, Mashhad, Iran; ^dMedical Chemistry Department, School of Pharmacy, Mashhad University of Medical Sciences, Mashhad, Iran; ^eEndoscopic and Minimally Invasive Surgery Research Center, Mashhad University of Medical Sciences, Mashhad, Iran

Communicated by Ramaswamy H. Sarma

ABSTRACT

The binding of small molecules with histone-DNA complexes can cause an interference in vital cellular processes such as cell division and the growth of cancerous cells that results in apoptosis. It is significant to study the interaction of small molecules with histone-DNA complex for the purpose of better understanding their mechanism of action, as well as designing novel and more effective drug compounds. The fluorescence quenching of ct-DNA upon interaction with Berberine has determined the binding of Berberine to ct-DNA with $K_{sv} = 9.46 \times 10^7 \text{ M}^{-1}$. K_{sv} value of ct-DNA-Berberine in the presence of H1 has been observed to be $3.10 \times 10^7 \text{ M}^{-1}$, indicating that the H1 has caused a reduction in the binding affinity of Berberine to ct-DNA. In the competitive emission spectrum, ethidium bromide (EB) and acridine orange (AO) have been examined as intercalators through the addition of Berberine to ct-DNA complexes, which includes ctDNA-EB and ctDNA-AO. Although in the presence of histone H1, we have observed signs of competition through the induced changes within the emission spectra, yet there has been apparently no competition between the ligands and probes. The viscosity results have confirmed the different behaviors of interaction between ctDNA and Berberine throughout the binary and ternary systems. We have figured out the IC50 and viability percent values at three different time durations of interaction between Berberine and MCF7 cell line. The molecular experiments have been completed by achieving the results of MTT assay, which have been confirmed to be in good agreement with molecular modeling studies.

Abbreviations: (Berberine): Berberine chloride; (EB): Ethidium Bromide; (AO): Acridine Orange

ARTICLE HISTORY

Received 15 December 2018
Accepted 21 January 2019

KEYWORDS

DNA interaction; Berberine chloride; spectroscopy; molecular modeling; cell culture; MTT assay; linker histone

1. Introduction

Cancer is acknowledged as the collapse of cellular regulation and uncontrolled cell division. DNA carries unique genetic information about all the living creatures and controls cellular regulations, which acts as the guiding agent for the biological procedures of cells that result in transcription replication and protein synthesis (Agarwal, Jangir, & Mehrotra, 2013; Anbazhagan & Renganathan, 2008; Arrondo, Muga, Castresana, & Goñi, 1993; Asadi, Safaei, Ranjbar, & Hasani, 2004). Cell DNA is known as the compact form of chromatin, and among the group of proteins called histones, which are involved in the formation of chromatin, histone H1 is labeled as their most important member. Hence, the DNA and histone-DNA complex have the potential of being utilized as therapeutic goals for designing anticancer drugs (Bazett-Jones, Côté, Landel, Peterson, & Workman, 1999).

Generally, there are three different ways that the anti-cancer drugs can interact with DNA including binding to DNA groove (groove binding interaction), the binding between two strands of DNA (intercalation interaction) and covalent binding. Drugs with intercalation interactions can eliminate the cancer cells by creating a binding between two DNA strands (Bera, Sahoo, Ghosh, & Dasgupta, 2008; Bi et al., 2006; Blake et al., 1999; Borchman, Yappert, & Herrell, 1991; Burton et al., 1978; Cao & He, 1998; Chen et al., 2005; Chi & Liu, 2011; Du et al., 2011; Sowrirajan, Yousuf, & Enoch, 2014). We have investigated the interaction of Berberine chloride with DNA and histone H1-DNA complex throughout this study. Berberine ($\text{C}_{20}\text{H}_{18}\text{NO}_4$) is a chemical compound with the molar mass of 366.36122 g/mol (Figure 1) (Gallori et al., 2000; Gittelsohn & Walker, 1967; Guo, Yue, & Gao, 2011; Hossain & Kumar, 2009; Huang & Zou, 2006; Ivankin, Carson, Kinney, & Wanunu, 2013; Jordan & Wilson, 2004; Kashanian

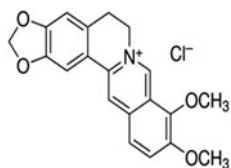


Figure 1. Chemical structure of Berberine chloride.

et al., 2008; Khare & Pande, 2012; Kumar, Naik, Girija, Sharath, & Pradeepa, 2012; Kypr & Vorlíčková, 2002; Lerman, 1961). It has been widely studied as an isokoinoline alkaloid that belongs to the Protobebine structural class and contains a cholesterol-like construction. In accordance with the available data, Berberine is capable of various biological and clinical activities such as antimicrobial, anticancer, anti-inflammatory and antioxidant effects (Li & Dong, 2009; Macquet & Butour, 1978; Nafisi, Saboury, Keramat, Neault, & Tajmir-Riahi, 2007; Neelam, Gokara, Sudhamalla, Amooru, & Subramanyam, 2010). This particular substance can induce apoptosis through NF κ B pathway and inhibit cell proliferation, as well as prevent and cause a delay in the progress of angiogenesis (Oohara & Wada, 1987). In addition, Jin et al. have studied the outcomes of Berberine on SKOV3 cancer cell line and reported that it has shown antitumor effects (Jin, Zhang, & Li, 2015). Berberine is also carried out to inhibit cancer cell proliferation by reducing the expression of BCL2 anti-apoptotic genes and increasing the expression of proapoptotic genes. Moreover, this interesting substance can induce apoptosis in the MCF-7 breast cancer cell line by causing a decrease in the expression of BCL2 and increasing the expression of CytC genes. Berberine has been widely studied and proven to contain antioxidant, antibacterial, anti-TB and antitumor properties (Tang et al., 2009).

In this research, we have performed investigations on the type of interaction between Berberine chloride with DNA and histone H1–DNA complex throughout a variety of methods including fluorescence spectroscopy, absorption spectroscopy, resonance light scattering, circular dichroism (CD), melting temperature measurement, viscosity measurements, molecular modeling and 3-(4,5-cimethylthiazol-2-yl)-2,5-diphenyl tetrazolium bromide (MTT) assay.

2. Materials and methods

2.1. Experimental section

Calf thymus DNA, histone H1 (Mw = 21500 g/mol), Berberine chloride (Mw = 371/81 g/mol), ethidium bromide (EB), and acridine orange (AO) have been purchased from Sigma-Aldrich Corporation (St. Louis, MO). Tris–HCl (>99%) has been procured from Merck Chemical Co. (Kenilworth, NJ).

DNA concentration has been determined spectrophotometrically. We have utilized the molar extinction coefficients of ctDNA ($\epsilon = 6600 \text{ M}^{-1} \text{ cm}^{-1}$ at 260 nm, $T = 298 \text{ K}$) for the purpose of estimating the concentration by the means of absorption measurements. Berberine chloride (0.025 mM) has been dissolved in dimethyl sulfoxide (DMSO) due to its very low solubility in water. All of the involved experiments have

been conducted in Tris–HCl buffer medium (10 mM) at pH 6.8.

The pH of the medium has been adjusted by the usage of citric acid, while the pH values of the solutions have been measured and stored at -4°C in the dark. The filtered DNA solution in the buffer has resulted in an ultraviolet (UV) absorbance ratio (A_{260}/A_{280}) of ~ 1.8 , which indicates that the DNA has been sufficiently freed from proteins. The interaction has been compared to the classical planar double-stranded DNA intercalator, EB and AO.

The stock solution ($25 \times 10^{-3} \text{ mM}$) of Berberine has been prepared in DMSO, while the calf thymus DNA (Sigma Chemical Co., St. Louis, MO) has been applied without any farther purification, and its stock solution has been composed by dissolving an appropriate amount of ctDNA in a Tris–HCl buffer solution. In the following, the solution has been allowed to rest overnight, and for a period of 1 week, it has been stored at 4°C in the dark. We have determined the concentration of ctDNA in the stock solution by means of UV absorption at 260 nm, which involved the application of molar absorption coefficient of $\epsilon_{260} = 6600 \text{ L.cm}^{-1}$ (Sohrabi, Hosseinzadeh, Beigoli, Saberi, & Chamani, 2018).

The purity of ctDNA has been confirmed by revealing the ratio of absorbance at 260 nm, in regard to the one at 280 nm. The solution has displayed a ratio of >1.8 at A_{260}/A_{280} , which indicates that the DNA has been sufficiently freed from proteins (Wang, Wang, Kollman, & Case, 2006). The EB and AO stock solutions (0.1 and 0.15 mM) have been prepared by dissolving their crystals (Sigma Chemical Co.) in a Tris–HCl buffer solution and having it stored in a cool and dark place.

We have recorded the absorption spectra on a Jasco UV–visible (Model V-60) spectrophotometer by means of a temperature controller in a quartz cuvette with 1 cm path length at 298 K. These particular spectra have been recorded for the free ctDNA and various Berberine–ctDNA in the absence and presence of H1 complexes solution. All of the fluorescence measurements have been carried out by the utilization of a Hitachi F-2500 spectrofluorimeter. All the measurements have been performed by keeping an excitation and emission band pass of 3 nm at $20 \pm 1.0^\circ\text{C}$.

Berberine solution (0.025 mM) has been appended to a 1.0 cm quartz cuvette and titrated by the successive addition of ctDNA for the purpose of obtaining a concentration of 10^{-5} mM . The solution has been allowed to rest for 5 min to equilibrate, and thus, the emission spectra have been recorded at 208, 303 and 308 K in the wavelength range of 375–650 nm. The appropriate blanks that corresponded to the Tris–HCl buffer solution have been subtracted to be corrected for the background fluorescence.

All of the fluorescence intensities have been corrected for the absorption of excited light and the re-absorption of emitted light. The following relationship has been used to correct the inner-filter effect (Wang et al., 2006)

$$F_c = F_m e^{(A_1 + A_2)/2} \quad (1)$$

where F_c and F_m stand for the corrected and measured fluorescence, respectively, while A_1 and A_2 represent the

absorbance of ctDNA at excitation and emission wavelengths, respectively.

All of the CD experiments have been conducted at 10 °C on a Jasco J-815 spectropolarimeter that had been equipped with a thermoelectrically controlled cell holder. The CD spectra have been recorded as an average of five scans from 300 to 200 nm in 0.1 nm increments. The initial DNA solution has been allowed to equilibrate for at least 30 min prior to the first session of drug addition.

The viscosity measurements have been conducted by the usage of an Ubbelohde viscometer (class company, Shanghai, China), which had been installed vertically in a constant temperature bath set at 2.5 ± 1 °C. While the volume of ctDNA solution has been kept at 15.0 ml, we have measured the flow time of the solution through the capillary by the employment of a digital stopwatch with an accuracy of p0.025. The means of five replicated measurements have been considered to estimate the viscosity of the samples.

MCF7 cell lines have been purchased from Buali Institute (Mashhad, Iran). Initially, they have been cultured in a DMEM that had been supplemented with 10% FBS, 1% penicillin and 1% streptomycin, which have been later on incubated at 37 °C in a humidified 5% CO₂ incubator. Complex solutions have been prepared immediately as a stock in H₂O before being applied. The Berberine has been added to the MCF7 cell line and incubated for the appointed time periods. We have procured the MCF7 cell line from the Cell Bank, Buali Institute (Mashhad, Iran), which was mammary gland, breast, derived from metastatic site (ATCC® HTB-22™). All of the involved reagents and mediums throughout this study have been prepared immediately before being applied.

The cells have been cultured in a DMEM (Gibco, Germany) that had been supplemented with 10% FBS (Gibco, Germany), penicillin (1% v/v) and streptomycin (1% v/v) at 37 °C in 5% CO₂ until reaching confluent. The effects of Berberine on the viability of MCF7 cells have been determined by means of MTT assay (Sigma-Aldrich, St. Louis, MA). Briefly, an initial population of 5000 cells/ml has been plated into each well of a 96-well culture plate that contained 100 µl aliquots of growth medium, which have been later on incubated for 48 h. 0.05 mg/ml of Berberine has been added to each well in triplicate of MCF7 or normal cells, and subsequent to 24 h of incubation, 5 mg/ml of MTT solution has been appended to the culture plates to achieve the final concentration of 0.5 mg/ml. In the following, the plates have been incubated for 3.5 h at 37 °C and thus had the precipitated formazan dissolved with 200 µl of DMSO. Through the application of an ELISA plate reader (Anthos, Australia), the absorbance has been observed to be at 490 nm. The IC₅₀ has been measured in the form of mg/ml.

2.2. Molecular docking

The structures of receptors (ctDNA and histone) have been procured from the Protein Data Bank. We have selected the 1BNA PDBID for the purpose of enquiring into the interactions of ctDNA Berberine. For the purpose of composing a receptor to evaluate the interactions of Berberine with

ctDNA–H1 complex, we have utilized a docked structure of histone and ctDNA with the accession codes of5NLO and 1BNA, respectively. The docking process of histone and ctDNA has been carried out in HEX8, while the correlation type has been set on the 'shape only'. In addition, the receptor and ligand have been given a twist range of 360° and a rotation range of 180°. The final docking results have been considered as the receptor for studying the interaction of Berberine with ctDNA–H1 (Berendsen, van der Spoel, & van Drunen, 1995; Sohrabi et al., 2018).

We have performed the structure preparations by means of MOE 2015.10 for receptors, which included the structural issue corrections, polar hydrogen addition and energy minimization. The structure of Berberine has been drawn in Chem Office®, while its energy has been minimized by the usage of AmBerberine10 force field that involved MOE 2015.10. Moreover, the docking assessments have been done by the same software that had been utilized when the entire receptor atoms had been set as the binding sites. London dG has been designated as the scoring matrix, whereas the best 100 poses of placements have been refined and analyzed for further studies.

2.3. Molecular dynamics (MD) simulations

The final docking results have been introduced to GROMACS-2018 (Wang, Wolf, Caldwell, Kollman, & Case, 2004) package for stability studies. The ligand parameters have been driven from Generalized AmBerberine Forcefield (GAFF) (Cornell et al., 1995), which is associated with the AntichamBerberine package on acpype web server (Coutsias, Seok, & Dill, 2004). Next to adding the partial charges of AM1-BCC, all of the ligand and receptor parameters have been set on the AmBerberine 99SB (Paul & Guchhait, 2011) Forcefield (Cornell et al., 1995). The docked structures have been positioned within a cubic box that had a minimum distance of 1 nm from the edge of neighboring box. To continue the procedure, an explicit TIP3P water model has been appended, and the systems have been neutralized by the sufficient amount of counter ions numBerberine. The steepest descend algorithm of minimization has been applied for the purpose of relaxing the system. Temperature and pressure equilibrations have been carried out in 100 ps to optimize thermodynamics parameters before the MD simulations. Finally, we have performed the MD simulations in 50 ns and analyzed the trajectories. By the application of excel, we have plotted the root-mean-square deviations (RMSDs) (Ghosh, Kundu, Paul, & Chattopadhyay, 2014) of ctDNA helical structure, which are relative to the reference structures and alpha carbons of the histone, for the purpose of estimating the structural stability throughout the course of the entire simulation time. The secondary structure analysis of histone, in the presence and absence of Berberine, has been carried out by the usage of DSSP program and plotted in Grace® software in regard to the last 5 ns of the simulations.

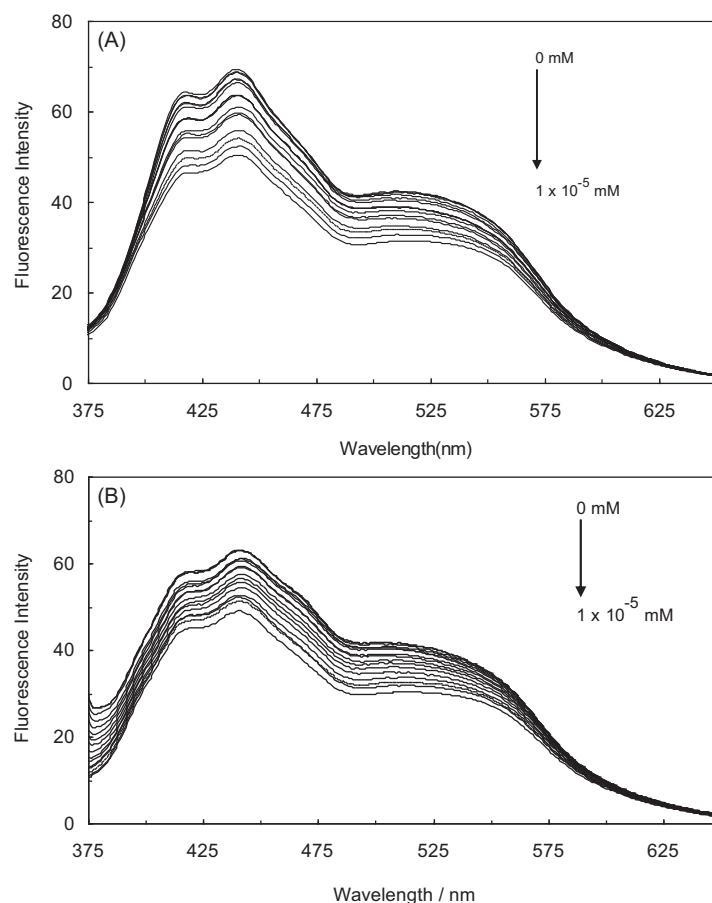


Figure 2. (A) Fluorescence emission spectrum of the Berberine complex in the presence of increasing amounts of ctDNA; (B) the ctDNA–H1 complex.

Table 1. The binding constants, thermodynamic parameters and Stern–Volmer dynamic quenching constants of ctDNA and H1–DNA with Berberine at different temperatures.

System	T/K	K_{sv}/M^{-1}	$\Delta G^{\circ}/kJ. mol^{-1}$	$\Delta H^{\circ}/kJ. mol^{-1}$	$\Delta S^{\circ}/J. mol^{-1}K^{-1}$
Ber–ctDNA	298	$(9.46 \pm 0.03) \times 10^7$	–45.51	–95.33	–167.08
	303	$(5.76 \pm 0.03) \times 10^7$	–45.01		
	308	$(2.41 \pm 0.03) \times 10^7$	–43.53		
Ber (H1–ctDNA)	298	$(3.1 \pm 0.03) \times 10^7$	–42.74	170.11	714.05
	303	$(8.85 \pm 0.03) \times 10^7$	–46.11		
	308	$(9.2 \pm 0.03) \times 10^7$	–49.91		

In conclusion, snapshots of the last picoseconds of simulations have been converted to pdb format and evaluated by means of MOE to obtain detailed structural interactions.

3. Results and discussion

3.1. Fluorescence spectroscopic measurements

To elucidate the mode of interaction, we have investigated the fluorescence quenching of DNA bounded to Berberine, which is in relation to the fluorescence quenching of Berberine in the buffered aqueous solution (see Figure 2(A and B)).

It should be noted that the protection of fluorophore from the quencher throughout the two different possible locations of the entrapped Berberine, including within the DNA double strands in the case of intercalative binding and the deep major or shallow minor grooves in groove binding,

is expected to be stronger in the former core and weaker in the latter situation (Daniel et al., 2015).

The quenching constants can be analyzed in accordance with the Stern–Volmer equation (Shahabadi, Hadidi, & Taherpour, 2014)

$$F_0/F = 1 + K_{sv} [Q] = 1 + k_q \tau_0 [Q] \quad (2)$$

where F_0 and F stand for the fluorescence intensities in the absence and presence of ctDNA and ctDNA–H1, respectively, K_{sv} would be the Stern–Volmer dynamic quenching constant, k_q is the quenching rate constant representing the average lifetime of the fluorescence molecules without ctDNA and ctDNA–H1 ($\tau_0 \approx 10^{-8}$) (Akbarabadi, Ismaili, Kahrizi, & Firouzabadi, 2018) and $[Q]$ stands for the concentrations of ctDNA and ctDNA–H1 complex.

Dynamic and static quenching can be distinguished through their different dependencies on temperature (Chi & Liu, 2011). K_q is the apparent biomolecular quenching rate

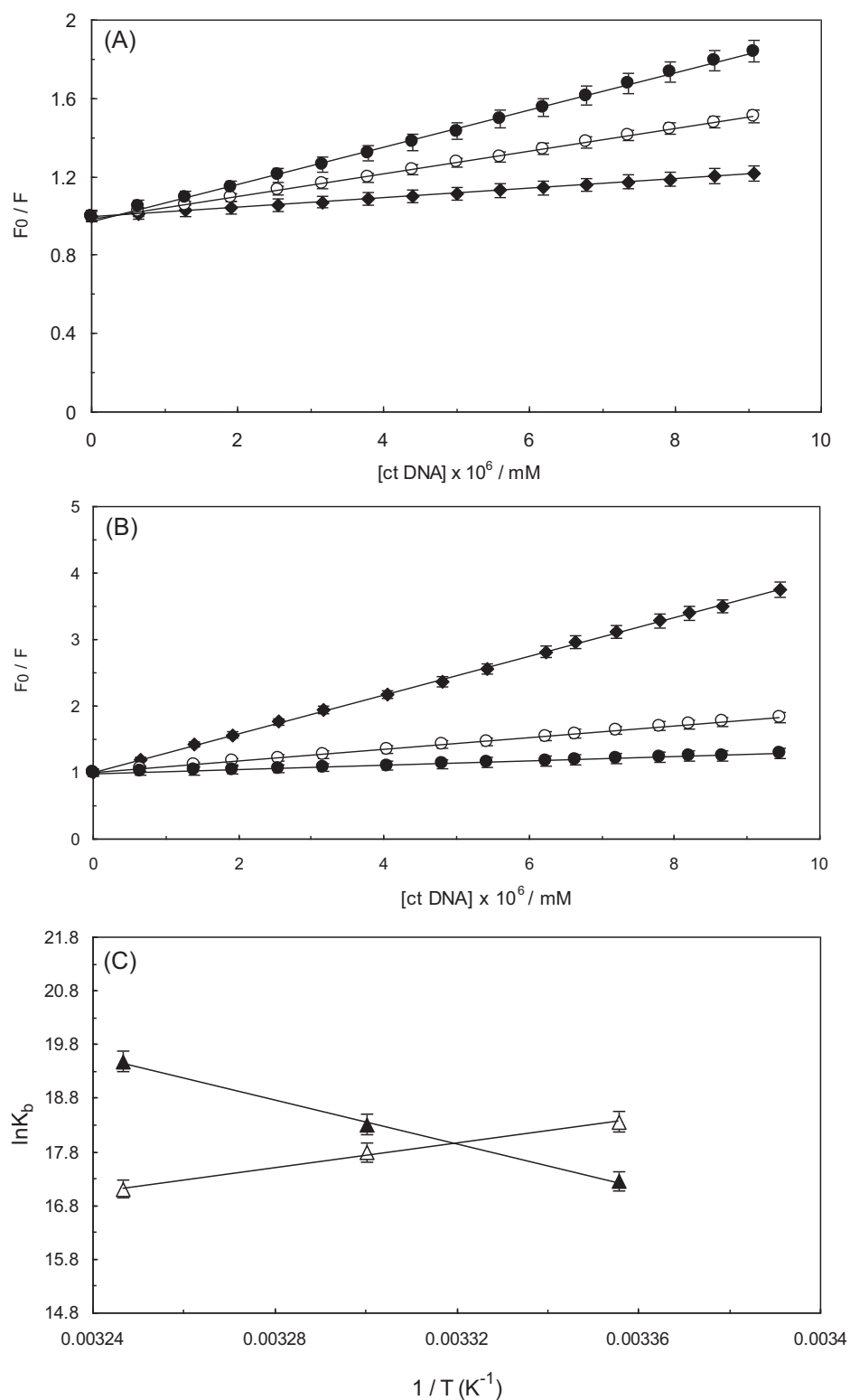


Figure 3. (A) The Stern–Volmer plots of Berberine quenching the fluorescence of ctDNA. (B) The H1–ctDNA complex, at three temperatures: 298 K closed circles; 303 K open circles; and 308 K closed diamonds, at pH = 6.8. (C) van’t Hoff plot for the interaction of ctDNA with Berberine (open triangle); the H1–ctDNA complex with Berberine (closed triangle).

constant, which is equaled to K_{sv}/τ_0 and in regard to dynamic quenching, the maximum scattering collision quenching constant of various quenchers is $2 \times 10^{10} \text{ L}\cdot\text{mol}^{-1}\text{s}^{-1}$. The obtained K_{sv} from Stern–Volmer equation at different temperatures are presented in Table 1 and Figure 3A and B.

As it can be observed, the K_{sv} values have increased as the temperature has been decreased throughout the formation of (ctDNA–H1) Berberine complex, which indicates that the mechanism of involved quenching may be the static kind, whereas in the case of ctDNA–Berberine complex, in the presence of H1 as the ternary system, the Stern–Volmer

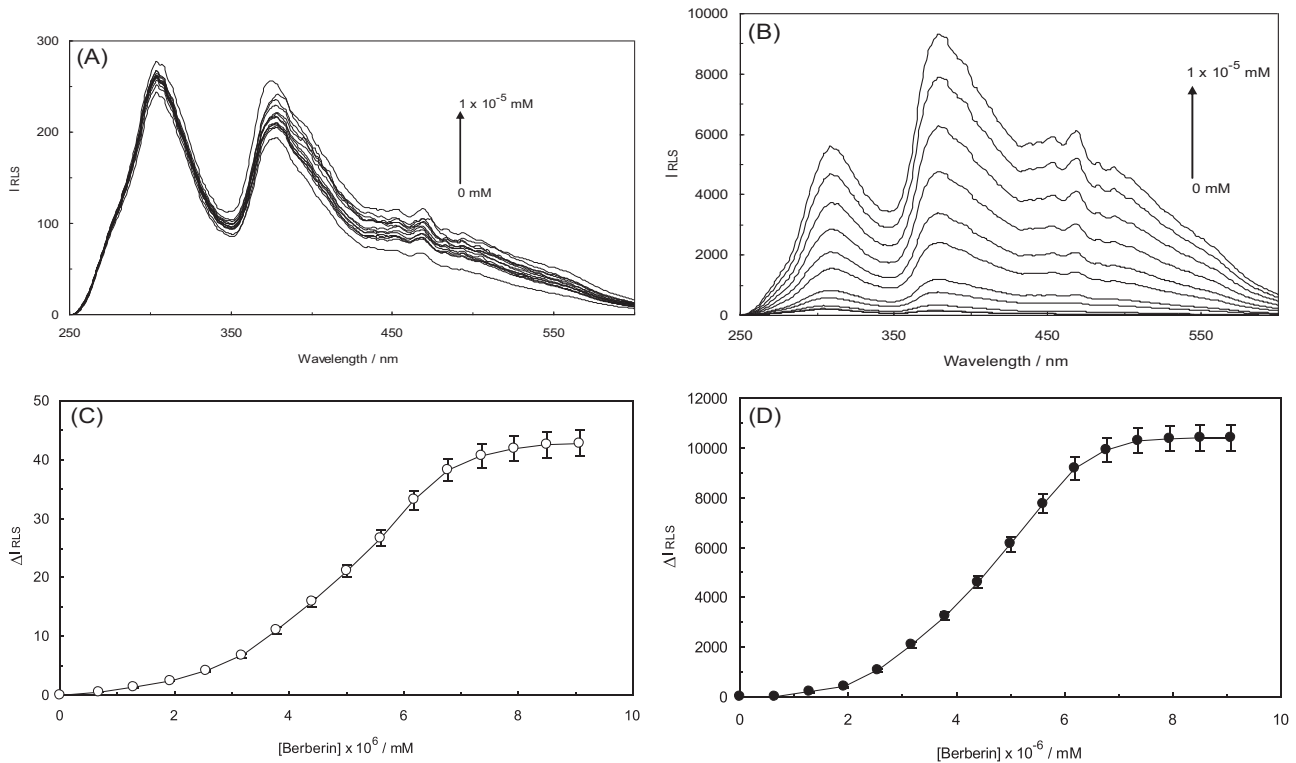


Figure 4. (A) The whole diffraction resonance and the interaction of Berberine with ctDNA; (B) H1-DNA complex at a temperature of 298 K and pH = 6.8; (C) ΔI_{RLS} curve against Berberine concentration of ctDNA–Berberine complex; (D) ΔI_{RLS} curve against Berberine concentration of (H1–ctDNA) Berberine complex.

constant (K_{SV}) has faced an increase from $(3.1 \pm 0.03) \times 10^7$ to $(9.2 \pm 0.03) \times 10^7$ as the temperature has been heightened from 298 to 308 K. These results have suggested that the probable quenching mechanism of Berberine by ctDNA, in the presence of H1, has involved the dynamic type, since the K_{SV} has been increased as a result of enhancing the temperature (Du et al., 2011).

Various types of non-covalent interactions, which can play a role in the binding procedure of a ligand to a biomolecule, include hydrogen bonds, van der Waals forces, and electrostatic and hydrophobic interactions. The binding constant, K_b , can be calculated through the following equation:

$$\log (F_0 - F)/F = \log K_b + n \log [Q] \quad (3)$$

The values of K have been obtained by plotting the values of $\log (F_0 - F)/F$ against $\log [Q]$ (figure not shown); the corresponding values are represented in Table 1.

The values of enthalpy and entropy changes have been calculated through the following equation:

$$\ln K = -\Delta H^0/RT + (\Delta S^0)/R \quad (4)$$

Utilizing the values of ΔH^0 and ΔS^0 , the values of ΔG^0 have been calculated by the following equation:

$$\Delta G^0 = \Delta H^0 - T \Delta S^0 \quad (5)$$

The corresponding values of ΔG^0 , ΔH^0 and ΔS^0 for the formation of ctDNA–Berberine complex, in the absence and presence of H1, are obtained from Figure 3C and listed in Table 1.

The results of this particular table have exhibited the crucial roles of van der Waals and hydrogen band throughout

the formation of ctDNA–Berberine complex as the binary system. In accordance with the thermodynamic data, the formation of ctDNA–Berberine complex is enthalpy-favored while being known to be entropy disfavored. The complex formation has been observed to result in a more ordered state, which is possibly caused by the freezing of motional freedom of Berberine and ctDNA molecules; therefore, the negative ΔS^0 value has confirmed the interactive mode of Berberine binding to ctDNA (Shakibapour, Dehghani Sani, Beigoli, Sadeghian, & Chamani, 2018). As it is demonstrated in Table 1, the values of ΔH^0 and ΔS^0 have been positive for the binding of Berberine to ctDNA in the presence of H1, which is regularly considered as an evidence of hydrophobic interaction. Hence, these observations have revealed the minor groove mode of interaction between Berberine and ctDNA, which has occurred in the presence of H1.

3.2. Resonance light scattering measurements

The resonance light scattering method is used to investigate the induced changes in molecular size, shape and weight of macromolecules, as well as the resulting complex (Aktipis & Panayotatos, 1976). As it is displayed in Figure 4A and B, the RLS intensity of ctDNA and the histone ctDNA–H1 complex have been intensified by enhancing the concentration of Berberine chloride in this experiment, which is due to the complex formation and conformational changes of ctDNA and ctDNA–H1.

Resonance light scattering represents the amount of light that had been scattered by the complex, since the larger the size of the particle is, the greater will be the dispersion of

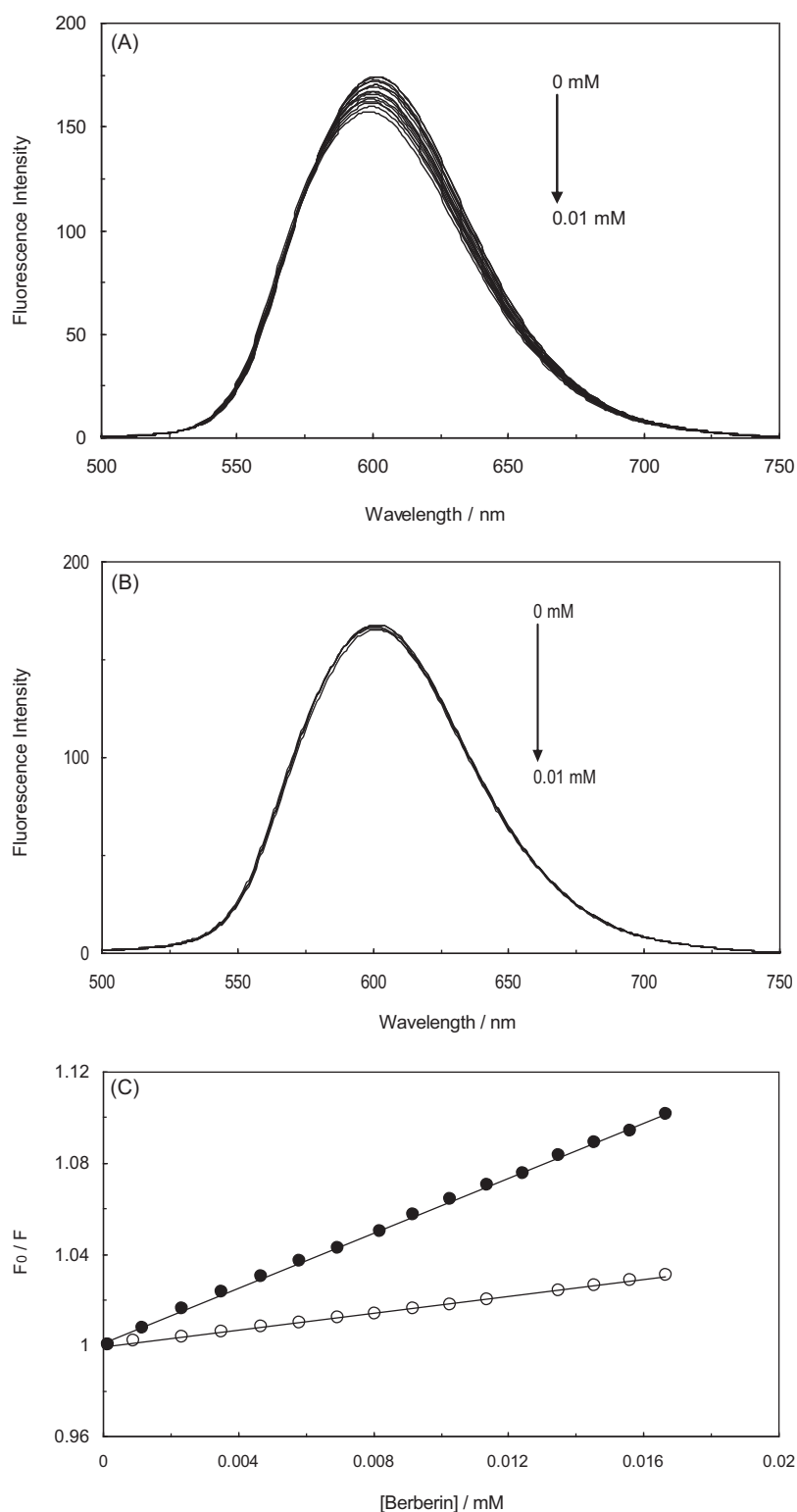


Figure 5. (A) Effect of Berberine in competition with ethidium bromide at an excitation wavelength of 440 nm upon interaction with ctDNA; (B) effect of Berberine in competition with ethidium bromide at an excitation wavelength of 440 nm upon interaction with H1-ctDNA complex; (C) Stern-Volmer plots of (ctDNA-EB) Berberine (closed circles) and (ctDNA-H1-EB) Berberine (open circles) complexes.

the sample size (Ma, Wang, & Zhang, 2017). It is possible to state two reasons for the observed increase in light diffraction, whereas one would be the increase of the soluble component and the other would be deposition, which is caused by the soluble component that is associated with the monomer state.

The RLS intensity is primarily dominated by the particle dimension of formed aggregate in the solution (Sarkar, Das, Basak, & Chattopadhyay, 2008). As it has been maintained by the results, it is assumed that ctDNA may interact with Berberine in the absence and presence of H1, leading to the genesis of new

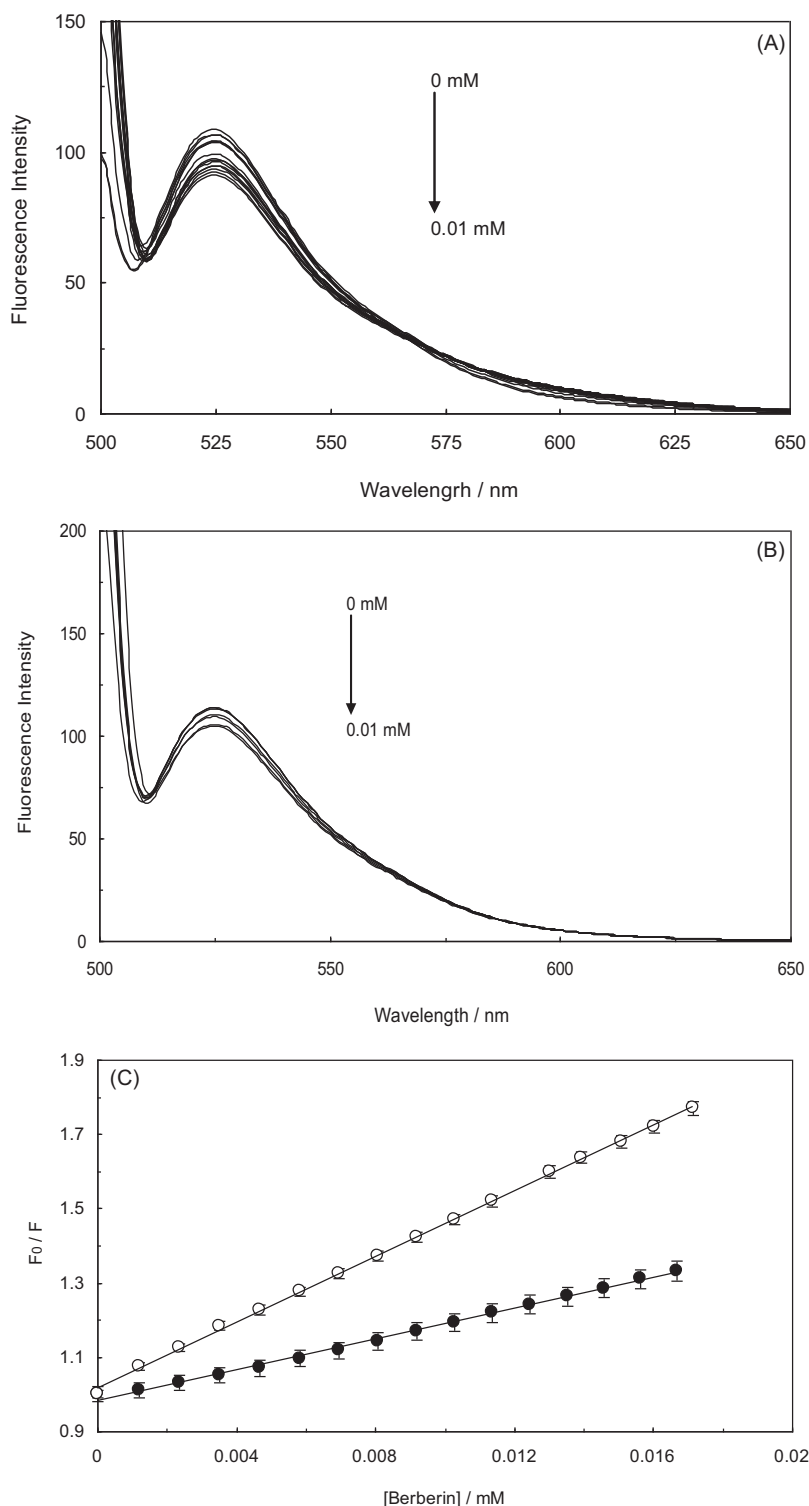


Figure 6. (A) Effect of Berberine in competition with acridine orange at an excitation wavelength of 351 nm upon interaction with ctDNA; (B) effect of Berberine in competition with acridine orange at an excitation wavelength of 351 nm upon interaction with (H1-ctDNA) complex; (C) Stern-Volmer plots of (ctDNA-AO) Berberine (closed circles) and (ctDNA-H1-AO) Berberine (open circles) complexes.

ctDNA-Berberine and (ctDNA-H1) Berberine complexes that could be expected to be an aggregate (see Figure 4C and D).

The size of ctDNA-Berberine and (ctDNA-H1) Berberine particles may be larger than that of Berberine, which could be the reason behind the increased light scattering signal under the given condition. Scientists have reported similar enhancement of RLS spectra upon

the aggregation of ligand onto both Z- and B-DNA (Sarkar et al., 2008).

3.3. Fluorescence spectra of competitive binding of berberine and EB for ctDNA and ctDNA-H1

In order to further study the binding mode, corresponding binding and thermodynamic parameters have been planned to be

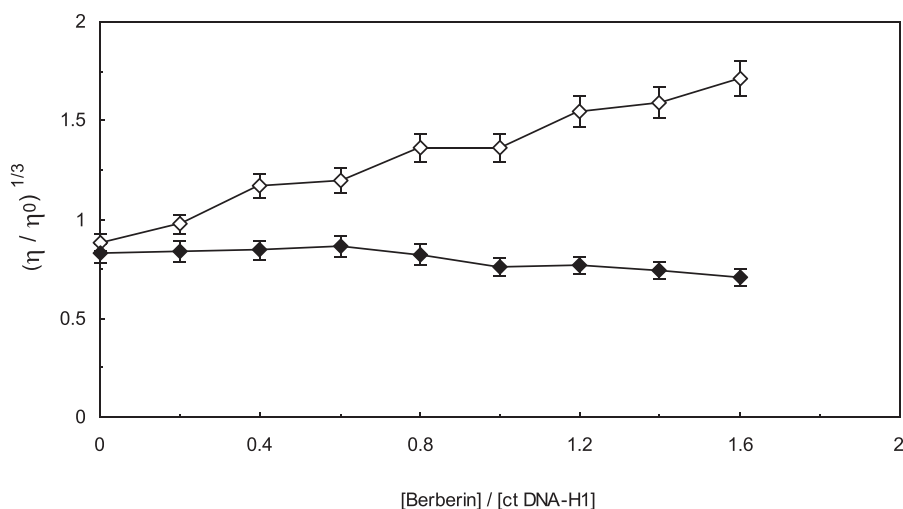


Figure 7. Effect of increasing amounts of Berberine on the relative viscosity of ctDNA (open diamonds) and ctDNA-H1 complex (closed diamonds) at pH = 6.8.

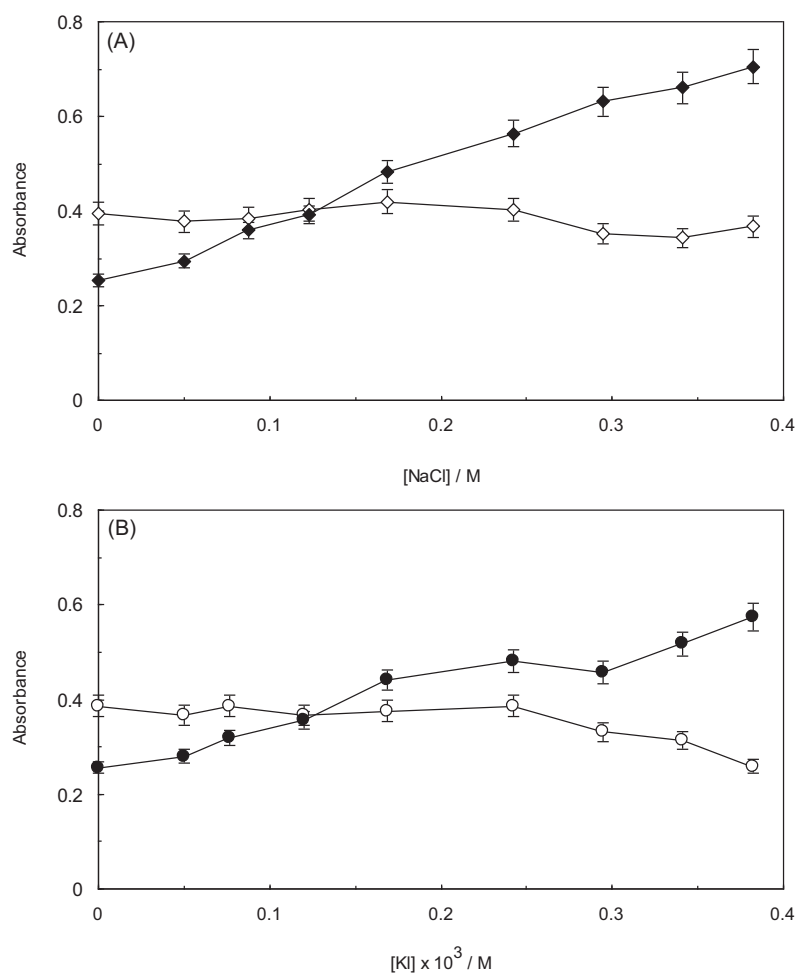


Figure 8. Effect of ionic strength of (A) NaCl on the fluorescence intensity of Berberine-ctDNA (closed diamonds) and Berberine (H1-ctDNA) complex (open diamonds); (B) KI on the fluorescence intensity of Berberine-ctDNA (closed circles) and Berberine (H1-ctDNA) complex (open circles).

determined by the utilization of fluorescence spectroscopy. The fluorescence intensity of EB seems to increase significantly after binding with DNA, which is apparently due to the induced interaction (Ross & Subramanian, 1981). If the Berberine molecules intercalate into the helix of DNA, they will display a competing behavior toward the EB in regard to the existing intercalation sites within the DNA, which can result in quenching the

enhanced fluorescence signal (Ross & Subramanian, 1981). Figure 5A represents the emission spectra of ctDNA-EB complex in the absence and presence of Berberine.

As it can be observed in the figure, this particular complex has displayed a strong fluorescence emission at 607 nm, upon being excited at 525 nm with the enhancement of Berberine, while its fluorescence intensity began to significantly decrease

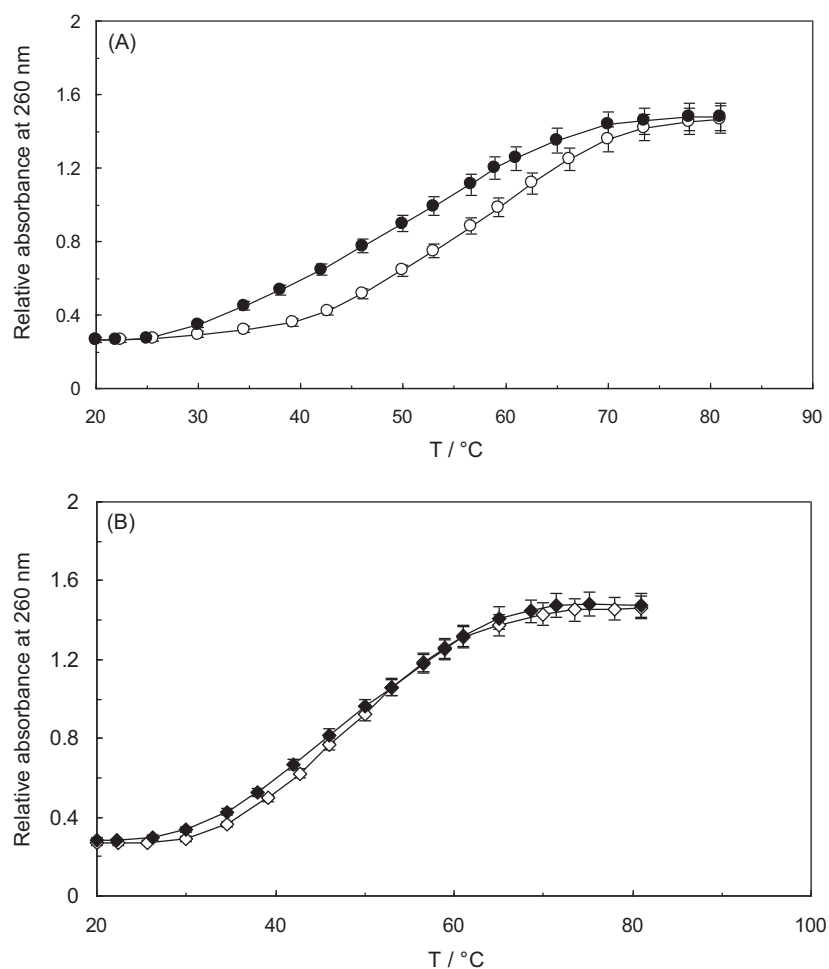


Figure 9. Melting curves of (A) ctDNA (closed circles), in the absence of Berberine; and (open circles), in the presence of Berberine; (B) (open circles) H1–ctDNA in the absence of Berberine; and (closed circles) in presence of Berberine at pH 6.8.

until reaching the initial intensity. This result has suggested that Berberine has apparently substituted for EB in the ctDNA–EB complex. The inset of Figure 5C illustrates the Stern–Volmer plot of (ctDNA–EB) Berberine, as well as the K_{sv} value ($6.02 \times 10^3 \text{ M}^{-1}$) that is associated with the existing interaction between ctDNA–EB and Berberine. The competitive binding of Berberine and EB to ctDNA–H1 has been evaluated in Figure 5B.

The interaction of EB with ctDNA–H1 has been characterized through the utilization of fluorescence spectra. An increase occurs throughout the fluorescence spectra of EB in the presence of ctDNA–H1, which is due to the higher planarity in the intercalation of ctDNA and its binding to H1. Upon the addition of Berberine to the appointed solution of (ctDNA–H1) EB complex, the fluorescence intensity has not been detected to change, indicating that Berberine has not exchanged with EB and the EB molecules have not been released into the solution subsequent to the induced interaction between ctDNA–H1–EB and Berberine. These observations have supported the hypothesis which states that Berberine is capable of interacting as a minor groove binder. Therefore, H1 can cause the binding site of Berberine to ctDNA by forming a complex with ctDNA. The Stern–Volmer curve of (ctDNA–H1–EB) Berberine is demonstrated in Figure 5C.

Figure 6A represents the emission spectra of interaction between ctDNA–AO and Berberine HCl. As it is perceived, a

reduction can be induced in the emission spectra of ctDNA–AO by increasing the concentration of Berberine HCl, which determines the enhancement of free AO concentration in the solution; hence, there is a comparison between Berberine HCl and AO within the binding site of ctDNA. AO is known to be an intercalator ligand that competes with Berberine HCl. Figure 6C displays the Stern–Volmer plot with the binding affinity of Berberine HCl to ctDNA–AO complex, and despite the noted fact, there has been no alterations throughout the emission fluorescence of (ctDNA–H1) AO complex that would determine the groove binding of Berberine HCl (Figure 6B).

3.4. Berberine chloride viscometer studies

Viscosity experiment is regarded as the most critical test for the binding mode of small molecules and DNA. Herein, the valuable investigations have determined that a classical intercalation binding demands for the space of adjacent base pairs to be large enough to accommodate the bound ligand and lengthen the double helix, which leads to the induction of a significant increase throughout the DNA viscosity (Haque, Bhuiya, Giri, Chowdhury, & Das, 2018). In order to further explore the binding of Berberine HCl to ctDNA and ctDNA–H1, viscosity measurements have been taken by

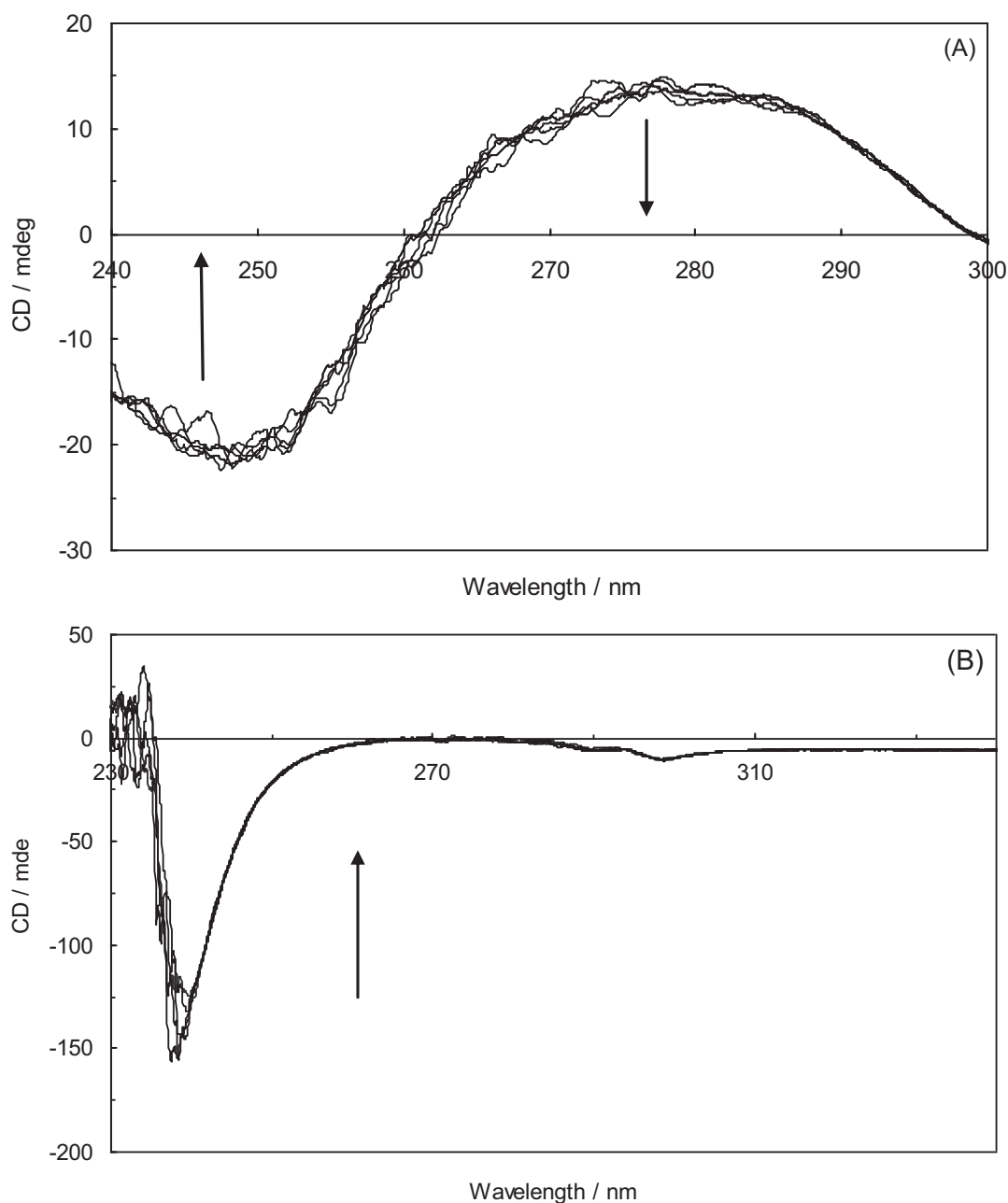


Figure 10. (A) Circular dichroism spectra of ctDNA; (B) H1-ctDNA complex, in the presence of different amounts of Berberine in 0.01-M Tris-HCl buffer (pH 6.8).

Table 2. Result of Berberine toxicity by MTT assay on MCF7 cell line in 0.05, 0.025, 0.0125 and 0.00625 M concentration at 24 h.

Minimum	43.6652 ± 6.867 (15.73%)
Maximum	152.632 ± 2294 (1503%)
IC ₅₀	$1.11455e-05 \pm 0.0007665$ (6877%)
Hill coefficient	0.62141 ± 3.903 (623.3%)

varying the concentrations of added Berberine HCl to ctDNA and ctDNA-H1 complex solutions. Figure 7 exhibits the alterations that have been observed in the relative viscosity of ctDNA and ctDNA-H1 in the presence of different concentrations of Berberine HCl. In accordance with this figure, the relative viscosities of ctDNA and ctDNA-H1 have remarkably increased and decreased by the enhancement of Berberine HCl concentration, respectively. This evidence has further confirmed that Berberine HCl can interact with ctDNA and ctDNA-H1 through the intercalative and groove binding modes, respectively.

Table 3. Result of Berberine toxicity by MTT assay on MCF7 cell line in 0.05, 0.025, 0.0125 and 0.00625 M concentration at 48 h.

Minimum	49.3217 ± 2.462 (4.992)
Maximum	104.696 ± 20.52 (19.6%)
IC ₅₀	0.000259227 ± 7542 (291.2%)
Hill coefficient	0.730547 ± 0.6755 (92.46%)

3.5. The effect of NaCl and KI on ctDNA-Berberine HCl and (ctDNA-H1) Berberine HCl

Electrostatic binding mode is known as one of the non-covalent binding modes of small molecules toward the DNA, which is often observed to function as an auxiliary in assisting groove binding and intercalation. The small molecule that binds strongly to DNA is usually accompanied by the electrostatic component. If the electrostatic binding interaction contains a dominant role throughout the binding

Table 4. Result of Berberine toxicity by MTT assay on MCF7 cell line in 0.05, 0.025, 0.0125 and 0.00625 M concentration at 72 h.

Minimum	44.0107 ± 2.57 (5.84%)
Maximum	104.766 ± 83.64 (79.83%)
IC ₅₀	0.000146653 ± 0.001632 (1113%)
Hill coefficient	0.9.6127 ± 2.595 (286.4%)

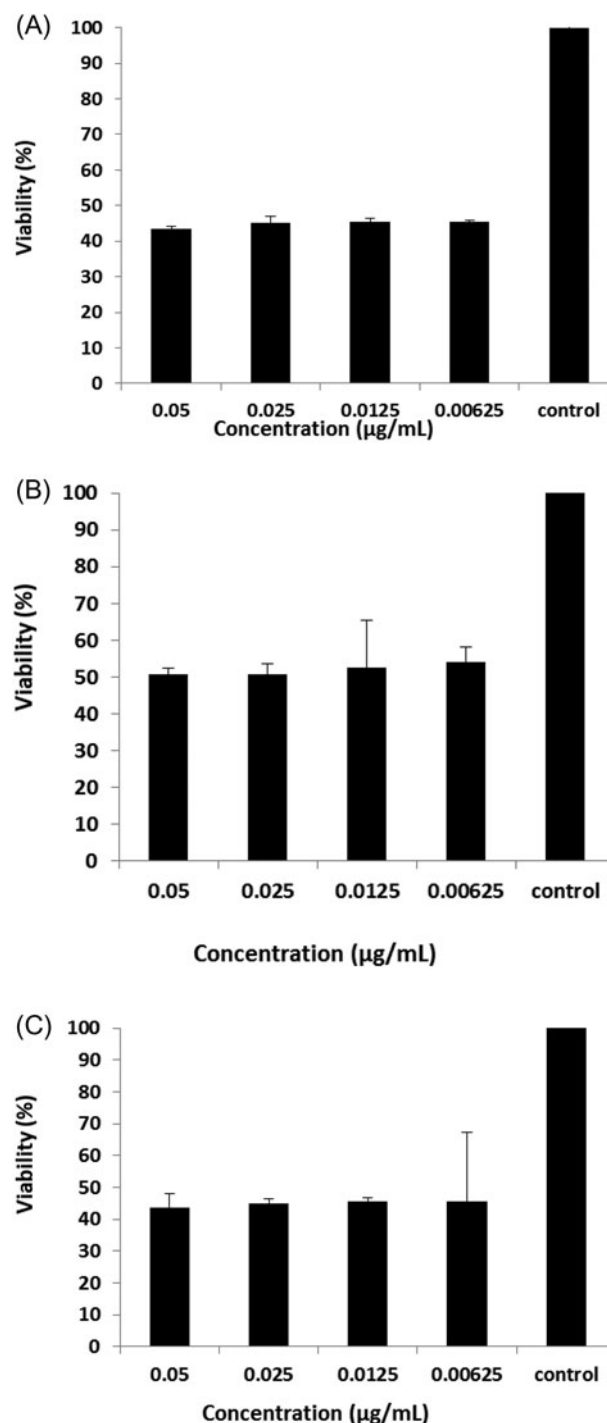
interaction of DNA with small molecules, the strength of interaction can be decreased by enhancing the salt concentration of the system (Huang et al., 2015). Figure 8A and B illustrates the experimental data in regard to the absorbance of ctDNA–Berberine HCl, which has apparently increased upon the addition of NaCl and KI concentrations, indicating that there has been an electrostatic binding interaction between ctDNA and Berberine HCl. On the other hand, the absorbance of ctDNA–Berberine HCl complex, in the presence of linker histone as the ternary system, has faced an increase as a result of enhancing the NaCl and KI concentrations, which appoints the lack of any existing significant electrostatic binding interaction between ctDNA and Berberine HCl. Therefore, it can be stated that linker histone plays an essential role throughout the formation of ctDNA–Berberine HCl complex. Moreover, it has been confirmed by the obtained results that linker histone can alter the behavior of ctDNA and Berberine interaction.

3.6. Transition point (T_m) studies

DNA denaturation, also called DNA melting, is a procedure where ds ctDNA unwinds and separates into ss ctDNA through the breakage of hydrogen bonding that has existed between the bases. Although the intercalation of small molecules into double helix can induce an increase in the melting temperature of DNA, yet the non-interaction binding has not caused any obvious heightening in the T_m (Ross & Subramanian, 1981). The melting point values of ctDNA, ctDNA–Berberine HCl, ctDNA–H1 and (ctDNA–H1) Berberine HCl have been determined by the employment of fluorescence spectroscopy method. For this matter, the fluorescence intensities of ctDNA, ctDNA–Berberine HCl, ctDNA–H1 and (ctDNA–H1) Berberine HCl have been noted down in the temperature range of 20–90 °C. The ctDNA and ctDNA–Berberine HCl melting curves, in the absence and presence of H1, are presented in Figure 9A, whereas the T_m value of ctDNA has been perceived to be increased by 4 °C (from 55 to 59 °C) as a result of binding to Berberine HCl and thereby confirming the intercalative mode of binding. It is displayed in Figure 9B that the enhancement of Berberine HCl concentration in the ctDNA–H1 solution has not caused an obvious increase in the T_m of the complex. The results have revealed that the binding mode of ctDNA–H1 with Berberine HCl has been non-intercalative and presumably consisted of groove binding mode.

3.7. CD spectra measurement

Considering its accuracy and sensitivity, CD is commonly utilized to monitor the conformational changes of protein and DNA. To diagnose the capability of Berberine HCl in inducing structural changes in ctDNA, we have measured the

**Figure 11.** Diagram of Berberine toxicity by MTT assay on MCF7 cell line in 0.05, 0.025, 0.0125 and 0.00625 M concentration at (A) 24, (B) 48 and (C) 72 h.

CD spectra of ctDNA and ctDNA–H1 complex in the absence and presence of Berberine HCl. As it is maintained by Figure 10A, ctDNA has displayed a negative band at 245 nm, caused by the right-handed helicity (Zavriev et al., 1979), and a positive band at 275 nm that has been induced by the base stacking (Kashanian & Ezzati Nazhad Dolatabadi, 2009); they have been the typical CD spectra of ctDNA classical B-conformation. In accordance with Figure 10A, the enhancement of Berberine HCl to ctDNA has caused a decrease in the intensity of negative band (shifting to zero levels), while the positive band has decreased without exhibiting any significant

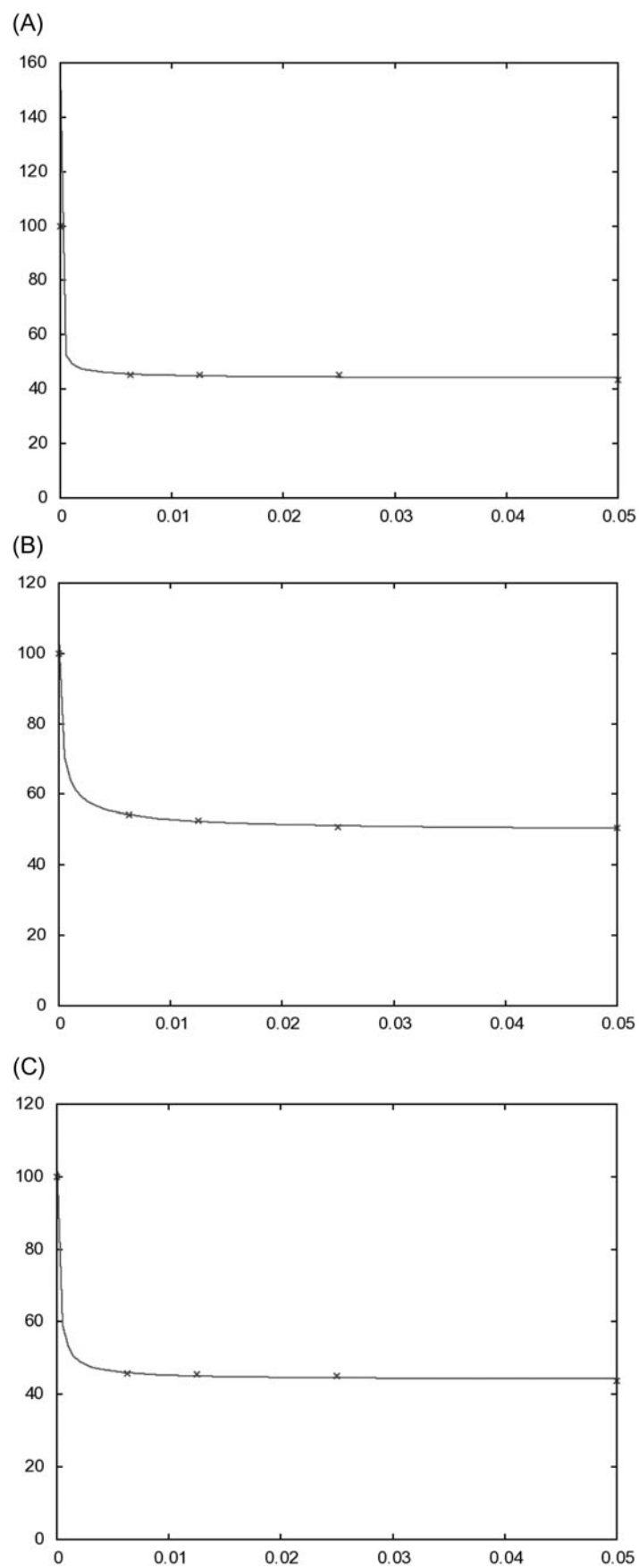


Figure 12. IC50 plot of Berberine toxicity by MTT assay on MCF7 cell line in 0.05, 0.025, 0.0125 and 0.00625 M concentration at (A) 24, (B) 48 and (C) 72 h.

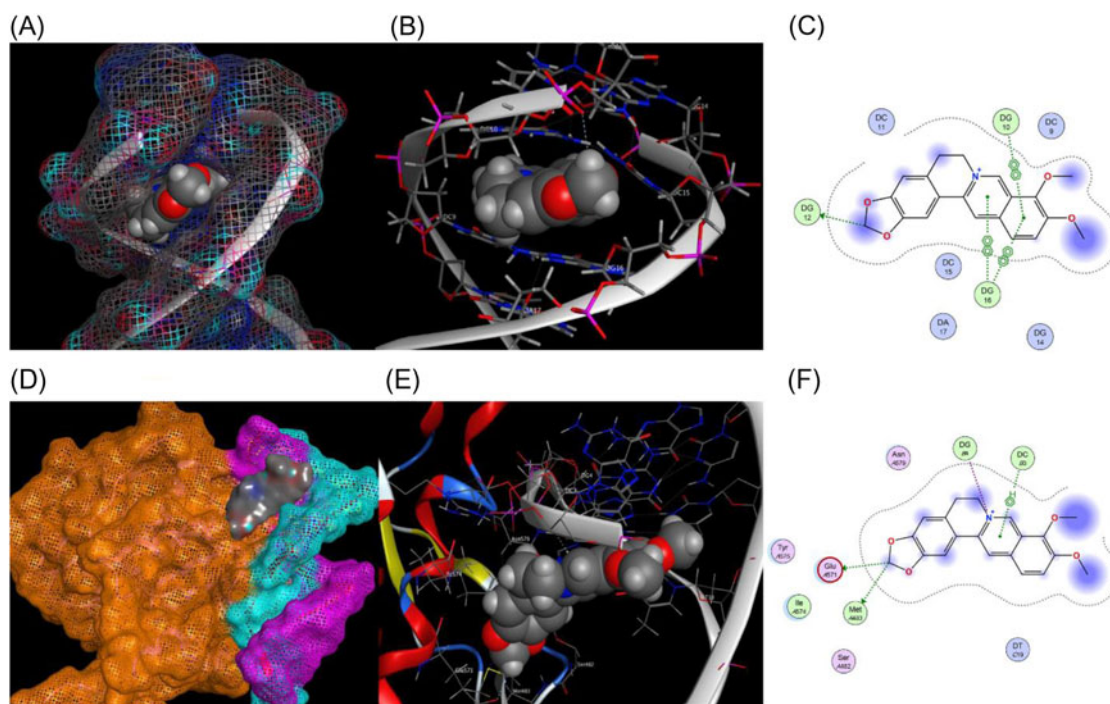


Figure 13. (A) Interaction of ctDNA with Berberine in a surface view, (B) atomic view, (C) 2D view, (D) interaction of ctDNA–H1 with Berberine in a surface view, (E) atomic view and (F) 2D view.

Table 5. Berberine interaction report with ctDNA–H1.

Berberine atoms	ctDNA–H1 atoms of residues	Interaction	Distance (Å)	Energy (kcal/mol)
C	SD of MET483	H-donor	3.61	–1.3
C	OE2 of GLU571	H-donor	3.38	–0.7
N	OP2 of G4	ionic	3.58	–1.6
6-ring	C2' of C3	π -H	4.44	–2.2

shifting. It has been indicated by the results that Berberine causes to induce the structural changes of ctDNA on the helix unwinding. Figure 10B illustrates the CD spectra of ctDNA–Berberine HCl in the absence and presence of H1. As it is maintained by this figure, the induced localized structural distortion in native B-DNA conformation suggests the perturbation of only few base pairs of DNA which has been observed where the binding of Berberine HCl has taken place. The local variations are of considerable significance for the occurrence of DNA–protein and DNA–ligand recognition process. The comparison between Figure 10A and B has revealed that H1 contains an important role in the formation of ctDNA–Berberine HCl complex, and therefore, H1 stands as a necessity for the correctness and fidelity of replication and transcription procedures.

3.8. MTT cytotoxicity assay

The cell viability of MCF7 cells has been determined through the utilization of MTT assay. 5000 cells per well have been seeded in 96-well plates, and after 24, 48 and 72 h, the culture media have been removed while the cells have been treated with the serial dilution of Berberine chloride at varying time intervals (Tables 2–4). Then, the MTT solution (4 mg/ml in PBS) has been added to each single well. Subsequent to 3 h of incubation at 37 °C at 5% CO₂, we have appended DMSO to each of the wells for the purpose of dissolving the formazan crystals.

Through the usage of a microplate reader (Epoch, USA), the absorbance of each well has been read at 570 and 630 nm, and the obtained results have been presented as a percentage of the control DMSO. The specific drug concentration that has inhibited cell proliferation up to 50% of the control DMSO (IC₅₀) has been determined from at least three independent experiments that had been performed in quadruplicate format throughout each treatment.

The cytotoxicity effects of Berberine on MCF7 cell line have been evaluated by the usage of MTT assay. As it is displayed in Figure 11, we have inhibited the cell growth through the performed treatment of MCF-7 cells by the application of different concentrations (0.025, 0.0125, 0.00625) for 24, 48, and 72 h. Figure 11A–C indicates that the cytotoxicity effect of Berberine on MCF-7 cell line is apparently dose-dependent and increases as the drug concentration is enlarged from 0.0625 to 0.05 molar cytotoxic properties at 24, 48, and 72 h.

Observation has proved that in the concentration of 0.05 μ g/ml, the death rate of MCF-7 breast cancer cell has been at its maximum point, while the cell survival rate has reached its lowest level.

The calculation of half-maximal inhibitory concentrations (IC₅₀) has been based on the dose–response curve that is displayed in Figure 12. The half-maximal inhibitory concentration of IC₅₀ stands as the designated volume of drug (mgr/ml), in which the growth and differentiation of 50% of the cancer cells is inhibited in comparison with the control cells that have not been affected by the drug.

3.9. MD simulations

To investigate and discover the best Berberine binding sites, we have considered assessing the free dockings that cover the

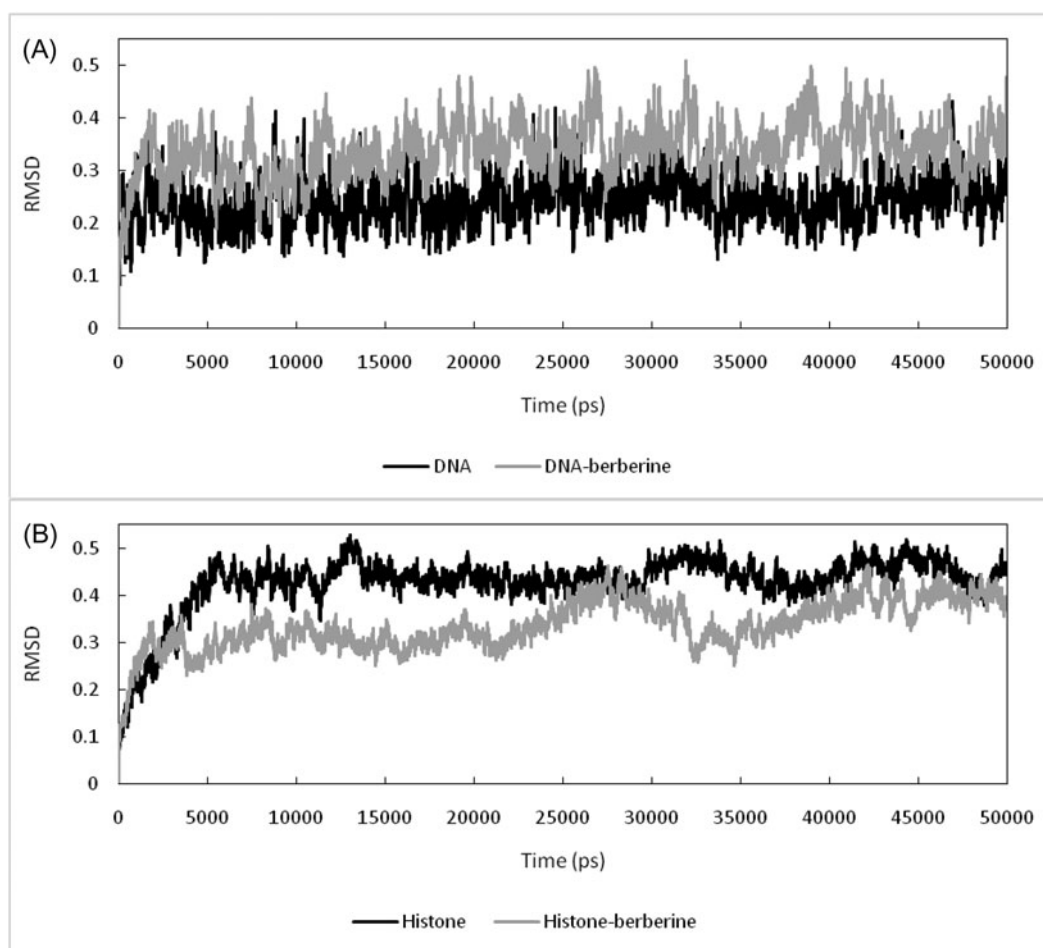


Figure 14. (A) RMSD of ctDNA before and after interaction with berberine from reference structures. (B) RMSD of C-alpha histone in ctDNA-H1 complex before and after interaction with berberine from reference structures.

entire receptor sites. All of the docking results have been apparent within the intercalation sites when ctDNA has functioned as the receptor. The averaged binding energy score has been observed to be -6.17 kcal/mol. Figure 13A–C displays the Berberine that existed in the intercalation site. The averaged distance of Berberine atoms from the ctDNA nucleotides has been around 3.7 Å. Most of the interactions have been perceived to be π -interactions (arene–arene), which have been induced between G10 and G16 of ctDNA and the aromatic rings of Berberine.

Upon the appointment of ctDNA-H1 as the receptor, Berberine has been observed to dock in diverse positions including histone superficial binding pockets, DNA groove binding sites and even the DNA intercalation sites. The averaged binding energy has been -4.16 kcal/mol. The best conformational structure with the minimum binding energy has been detected in the Berberine that had one of its sides located in the groove binding site, while the other was positioned in one of the histone cavities. In these specific circumstances, Berberine has displayed the most possible interactions. Figure 13D–F illustrates the Berberine that has been situated in the groove binding site of ctDNA-H1 receptor. In this figure, ctDNA-H1 has been colored based on the chains and location of Berberine within the histone cavity, while the ctDNA

groove binding site has been dominant. Berberine contains 2 H bond interactions with Met 483 and Glu 571 of histone, whereas on the other side, there is a potent ionic interaction between the G4 of ctDNA and N^+ of Berberine. In addition, one π -H interaction has occurred between C3 and aromatic rings of Berberine (Table 5).

The structural stabilities of the obtained docking results have been analyzed through the utilization of Gromacs. The outcomes of MD simulations have confirmed that Berberine has been capable of being completely stable in its active sites in the courses of 50 ns simulations. We have plotted the RMSD of ctDNA and histone, before and after the binding of Berberine, shown in Figure 14A and B.

The presence of Berberine in the intercalation site of ctDNA can apparently distort the helicity of DNA structure, and as it can be observed, the RMSD of ctDNA from reference structure has been reduced around 0.1 unit. However, the stability of proteins seems to increase a bit as the Berberine interacts with ctDNA-H1, which can be considered as a demonstration of a potent interaction between the histone and Berberine. In regard to this matter, the secondary structure analysis of histone throughout the last 5 ns of simulation has displayed the inducement of minimum changes in the secondary structures (Figure 15A and B).

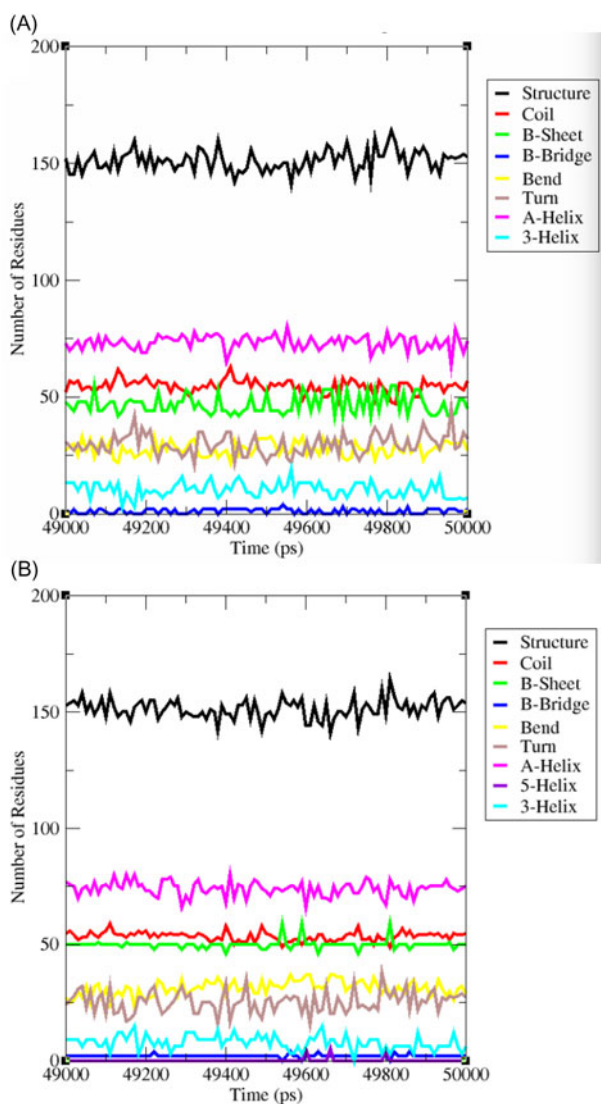


Figure 15. (A) Secondary structure of histone in the absence of Berberine in the last 5 ns of simulations. (B) Secondary structure of histone in the presence of Berberine in the last 5 ns of simulations.

4. Conclusion

In this article, we have studied the interaction of Berberine chloride with ctDNA and histone H1–ctDNA complex in the environment, containing a pH = 6.8, and physiological conditions through the employment of various methods such as spectroscopy, fluorescence spectrometry, resonance light scattering, temperature transfer study, viscometry, absorption spectroscopy and CD, along with molecular modeling and its effects on MCF-cell line. In order to perform investigations on the type of Berberine chloride interaction with histone complex H1–ctDNA, we have evaluated the interaction of this compound in inhibiting the DNA division and histone H1, which stand as the inhibitors of gene expression. The results of the published spectroscopy have indicated that the presence of DNA and histone complex H1–ctDNA can silence the release of ligand fluorophore. In the absence of histone H1, the slope has been observed to decrease as the temperature has been heightened, which suggests the existence of static interactions and possibly ligand binding between the two DNA strands. On the other hand in the presence of a

histone H1, an increase has been induced in the slope as the temperature has been heightened, which indicates the existence of dynamic interactions while its type of binding has been groove binding. Through the assistance of van't Hoff diagram, the thermodynamic quantities have been obtained in the presence of a histone H1. The enthalpy and entropy values have been negative in the absence of a histone H1, which indicates that the involved forces have been van der Waals and hydrogen bonds. However, in the presence of histone H1, the enthalpy and entropy values have been apparently positive, which determines that the major contribution of interactions has been hydrophobic and the type of interaction has been probably groove binding. In the course of the experiments that involved resonance light scattering with increasing diffraction, the ligand has provided the formation of a complex in the presence and absence of histone H1.

The performed investigation on the competitive interaction of Berberine chloride with EB and AO on the binding site to DNA has confirmed that Berberine chloride can separate the DNA probes, which proves that the type of interaction between DNA and Berberine chloride is probably the type of intercalation that exists between the two strands. However, in the presence of histone H1, the reduction in emission regarding the competition between the ligand and probe is much less than the amount of reduction in its absence, indicating that the type of interaction has changed in its presence. In the absence of histone H1 and the addition of ligands, viscometric studies have confirmed that an interaction exists between the two strands by observing an enlargement in viscosity. However, in the presence of histone H1, viscosity has not only increased but also decreased, which suggests that the type of interaction has been binding to the DNA groove. The performed investigations on the competition between salts and Berberine chloride have confirmed the mentioned results, since in the absence of histone H1, the ligand competes with both sodium chloride and potassium iodide and considering how salts are bounded between the two strands of ctDNA, the type of interaction in the absence of a histone H1 is apparently the binding between two strings. Nevertheless, the results have been different in the presence of histone H1, since there has not been any competition between Berberine chloride and salts due to ligand binding to the groove. Throughout the absence of a histone H1, the performed studies on temperature transfer have confirmed that the type of binding is between two strands, considering how the T_m has been observed to heighten; despite the mentioned fact, T_m has not been detected to change as much in the presence of histone H1. Longitudinal exponential doping tests, in the presence and absence of histone H1, have affirmed the mentioned results by displaying an increasing peak in the distant area and an enlargement throughout the near area.

All of the carried-out experiments have confirmed that the type of interaction between Berberine chloride and DNA is the type of inter-binding between the two strands, also known as the intercalator ligand. Moreover, the interaction

between Berberine chloride and histone H1–ctDNA complex is apparently the kind of binding to the ctDNA groove.

The results of cell culture and MTT test have proved that 0.00625 mM is the lowest concentration of ligand that has been effective in causing the proliferation of MCF7 cell, and it has been observed to intensify by increasing the applied concentration, which indicates that Berberine has showed cytotoxicity and caused the death of cancer cells by activating the apoptosis in living cells.

The results of molecular modeling have exhibited that the Berberine binding, in the absence of a histone H1, is a type of binding between the droplet, while in the presence of histone H1, it has been detected to be the type of binding to the DNA groove. All of the obtained results have signified that Berberine chloride can be positioned between the two DNA strands in the absence of histone H1, while in its presence, it binds to the DNA groove. In accordance with the outcomes of molecular modeling, Berberine chloride can also interact with histone H1 macromolecule.

Acknowledgements

The financial support of the Research Council of the Mashhad Branch, Islamic Azad University, is gratefully acknowledged. The authors thank Dr. Ljungburg for English editing.

Disclosure statement

No potential conflict of interest was reported by the authors.

References

- Agarwal, S., Jangir, D. K., & Mehrotra, R. (2013). Spectroscopic studies of the effects of anticancer drug mitoxantrone interaction with calf-thymus DNA. *Journal of Photochemistry and Photobiology. B, Biology*, 120, 177–182.
- Akbarabadi, A., Ismaili, A., Kahrizi, D., & Firouzabadi, F. N. (2018). Resistance determination of the ACCase-inhibiting herbicide of clodinafop propargyl in *Avena ludoviciana* (Durieu), and study of their interaction using molecular docking and simulation. *Molecular Biology Reports*, 1–10.
- Aktipis, S., & Panayotatos, N. (1976). Mechanism of ethidium bromide inhibition of RNA polymerase. *Biochemical and Biophysical Research Communications*, 68(2), 465–470. doi:10.1016/0006-291X(76)91168-2
- Anbazhagan, V., & Renganathan, R. (2008). Study on the binding of 2, 3-diazabicyclo [2.2. 2] oct-2-ene with bovine serum albumin by fluorescence spectroscopy. *Journal of Luminescence*, 128(9), 1454–1458. doi: 10.1016/j.jlumin.2008.02.004
- Arrondo, J. L. R., Muga, A., Castresana, J., & Goñi, F. M. (1993). Quantitative studies of the structure of proteins in solution by Fourier-transform infrared spectroscopy. *Progress in Biophysics and Molecular Biology*, 59(1), 23–56. doi:10.1016/0079-6107(93)90006-6
- Asadi, M., Safaei, E., Ranjbar, B., & Hasani, L. (2004). Thermodynamic and spectroscopic study on the binding of cationic Zn (II) and Co (II) tetrapyrroloporphyrazines to calf thymus DNA: The role of the central metal in binding parameters. *New Journal of Chemistry*, 28(10), 1227–1234. doi:10.1039/b404068f
- Bazett-Jones, D. P., Côté, J., Landel, C. C., Peterson, C. L., & Workman, J. L. (1999). The SWI/SNF complex creates loop domains in DNA and polynucleosome arrays and can disrupt DNA–histone contacts within these domains. *Molecular and Cellular Biology*, 19(2), 1470–1478. doi: 10.1128/MCB.19.2.1470
- Bera, R., Sahoo, B. K., Ghosh, K. S., & Dasgupta, S. (2008). Studies on the interaction of isoxazolcurcumin with calf thymus DNA. *International Journal of Biological Macromolecules*, 42(1), 14–21. doi:10.1016/j.ijbiomac.2007.08.010
- Berendsen, H. J., van der Spoel, D., & van Drunen, R. (1995). GROMACS: A message-passing parallel molecular dynamics implementation. *Computer Physics Communications*, 91(1-3), 43–56. doi:10.1016/0010-4655(95)00042-E
- Bi, S., Qiao, C., Song, D., Tian, Y., Gao, D., Sun, Y., & Zhang, H. (2006). Study of interactions of flavonoids with DNA using acridine orange as a fluorescence probe. *Sensors and Actuators B: Chemical*, 119(1), 199–208. doi:10.1016/j.snb.2005.12.014
- Blake, R. D., Bizzaro, J. W., Blake, J. D., Day, G. R., Delcourt, S. G., Knowles, J., ... SantaLucia, J. (1999). Statistical mechanical simulation of polymeric DNA melting with MELTSIM. *Bioinformatics (Oxford, England)*, 15(5), 370–375. doi:10.1093/bioinformatics/15.5.370
- Borchman, D., Yappert, M., & Herrell, P. (1991). Structural characterization of human lens membrane lipid by infrared spectroscopy. *Investigative Ophthalmology & Visual Science*, 32(8), 2404–2416.
- Burton, D., Butler, M., Hyde, J., Phillips, D., Skidmore, C., & Walker, I. (1978). The interaction of core histones with DNA: Equilibrium binding studies. *Nucleic Acids Research*, 5(10), 3643–3664. doi:10.1093/nar/5.10.3643
- Cao, Y., & He, X-W. (1998). Studies of interaction between safranin T and double helix DNA by spectral methods. *Spectrochimica Acta Part A: Molecular and Biomolecular Spectroscopy*, 54(6), 883–892. doi: 10.1016/S1386-1425(97)00277-1
- Chen, W.-H., Qin, Y., Cai, Z., Chan, C.-L., Luo, G.-A., & Jiang, Z.-H. (2005). Spectrometric studies of cytotoxic protoberberine alkaloids binding to double-stranded DNA. *Bioorganic & Medicinal Chemistry*, 13(5), 1859–1866. doi:10.1016/j.bmc.2004.10.049
- Chi, Z., & Liu, R. (2011). Phenotypic characterization of the binding of tetracycline to human serum albumin. *Biomacromolecules*, 12(1), 203–209. doi:10.1021/bm1011568
- Cornell, W. D., Cieplak, P., Bayly, C. I., Gould, I. R., Merz, K. M., Ferguson, D. M., ... Kollman, P. A. (1995). A second generation force field for the simulation of proteins, nucleic acids, and organic molecules. *Journal of the American Chemical Society*, 117(19), 5179–5197. doi: 10.1021/ja00124a002
- Coutsias, E. A., Seok, C., & Dill, K. A. (2004). Using quaternions to calculate RMSD. *Journal of Computational Chemistry*, 25(15), 1849–1857.
- Daniel, B., Pavkov-Keller, T., Steiner, B., Dordic, A., Gutmann, A., Nidetzky, B., ... Gruber, K. (2015). Structural and biochemical characterization of a monolignol oxidoreductase from *A. thaliana* implies a link between the berberine bridge enzyme-like family and cell wall metabolism. Paper Presented at the 13th DocDay-NAWI Graz Doctoral School of Molecular Biosciences and Biotechnology, Graz, Austria.
- Du, K.-J., Wang, J.-Q., Kou, J.-F., Li, G.-Y., Wang, L.-L., Chao, H., & Ji, L.-N. (2011). Synthesis, DNA-binding and topoisomerase inhibitory activity of ruthenium (II) polypyridyl complexes. *European Journal of Medicinal Chemistry*, 46(4), 1056–1065. doi:10.1016/j.ejmech.2011.01.019
- Gallori, E., Vettori, C., Alessio, E., Vilchez, F. G., Vilaplana, R., Orioli, P., ... Messori, L. (2000). DNA as a possible target for antitumor ruthenium (III) complexes. A spectroscopic and molecular biology study of the interactions of two representative antineoplastic ruthenium (III) complexes with DNA. *Archives of Biochemistry and Biophysics*, 376(1), 156–162. doi:10.1006/abbi.1999.1654
- Ghosh, S., Kundu, P., Paul, B. K., & Chattopadhyay, N. (2014). Binding of an anionic fluorescent probe with calf thymus DNA and effect of salt on the probe–DNA binding: A spectroscopic and molecular docking investigation. *RSC Advances*, 4(108), 63549–63558. doi:10.1039/C4RA14298E
- Gittelson, B., & Walker, I. (1967). The interaction of proflavine with deoxyribonucleic acid and deoxyribonucleohistone. *Biochimica et Biophysica Acta*, 138(3), 619. doi:10.1016/0005-2787(67)90563-1
- Guo, Y., Yue, Q., & Gao, B. (2011). Molecular docking study investigating the possible mode of binding of CI Acid Red 73 with DNA. *International Journal of Biological Macromolecules*, 49(1), 55–61. doi: 10.1016/j.ijbiomac.2011.03.009
- Haque, L., Bhuiya, S., Giri, I., Chowdhury, S., & Das, S. (2018). Structural alteration of low pH, low temperature induced protonated form of DNA to the canonical form by the benzophenanthridine alkaloid

- nitidine: Spectroscopic exploration. *International Journal of Biological Macromolecules*, 119, 1106–1112. doi:10.1016/j.ijbiomac.2018.08.031
- Hossain, M., & Kumar, G. S. (2009). DNA binding of benzophenanthridine compounds sanguinarine versus ethidium: Comparative binding and thermodynamic profile of intercalation. *The Journal of Chemical Thermodynamics*, 41(6), 764–774. doi:10.1016/j.jct.2008.12.008
- Huang, S., Zhu, F., Xiao, Q., Liang, Y., Zhou, Q., & Su, W. (2015). Thermodynamic investigation of the interaction between the [(η 6-p-cymene) Ru (benzaldehyde-*N*-4-phenylthiosemicarbazone) Cl] Cl anticancer drug and ctDNA: Multispectroscopic and electrochemical studies. *RSC Advances*, 5(53), 42889–42902. doi:10.1039/C5RA03979G
- Huang, S. Y., & Zou, X. (2006). Efficient molecular docking of NMR structures: Application to HIV-1 protease. *Protein Science*, 16(1), 43–51. doi:10.1110/ps.062501507
- Ivankin, A., Carson, S., Kinney, S. R., & Wanunu, M. (2013). Fast, label-free force spectroscopy of histone–DNA interactions in individual nucleosomes using nanopores. *Journal of the American Chemical Society*, 135(41), 15350–15352. doi:10.1021/ja408354s
- Jin, P., Zhang, C., & Li, N. (2015). Berberine exhibits antitumor effects in human ovarian cancer cells. *Anti-Cancer Agents in Medicinal Chemistry (Chemistry)*, 15(4), 511–516. doi:10.2174/1871520614666141226124110
- Jordan, M. A., & Wilson, L. (2004). Microtubules as a target for anticancer drugs. *Nature Reviews. Cancer*, 4(4), 253.
- Kashanian, S., Askari, S., Ahmadi, F., Omidfar, K., Ghobadi, S., & Tarighat, F. A. (2008). *In vitro* study of DNA interaction with clodinafop-propargyl herbicide. *DNA and Cell Biology*, 27(10), 581–586.
- Kashanian, S., & Ezzati Nazhad Dolatabadi, J. (2009). *In vitro* study of calf thymus DNA interaction with butylated hydroxyanisole. *DNA. Cell Biology*, 28(10), 535–540. doi:10.1089/dna.2009.0906
- Khare, D., & Pande, R. (2012). Experimental and molecular docking study on DNA binding interaction of *N*-phenylbenzohydroxamic acid. *Der Pharma Chemica*, 4(1), 66–75.
- Kumar, B. V., Naik, H. B., Girija, D., Sharath, N., & Pradeepa, S. (2012). Metal complexes of new tetraazamacrocyclic constrained oxadiazole ring as subunits: Synthesis, DNA binding and photonuclease activity. *Journal of Macromolecular Science, Part A*, 49(2), 139–148. doi:10.1080/10601325.2012.642210
- Kypr, J., & Vorlíčková, M. (2002). Circular dichroism spectroscopy reveals invariant conformation of guanine runs in DNA. *Biopolymers: Original Research on Biomolecules*, 67(4–5), 275–277. doi:10.1002/bip.10112
- Lerman, L. (1961). Structural considerations in the interaction of DNA and acridines. *Journal of Molecular Biology*, 3(1), 18
- Li, J., & Dong, C. (2009). Study on the interaction of morphine chloride with deoxyribonucleic acid by fluorescence method. *Spectrochimica Acta Part A: Molecular and Biomolecular Spectroscopy*, 71(5), 1938–1943. doi:10.1016/j.saa.2008.07.033
- Ma, L., Wang, J., & Zhang, Y. (2017). Probing the characterization of the interaction of aflatoxins B1 and G1 with calf thymus DNA *in vitro*. *Toxins*, 9(7), 209.
- Macquet, J. P., & Butour, J. L. (1978). A circular dichroism study of DNA-platinum complexes: Differentiation between monofunctional. cis-bidentate and trans-bidentate platinum fixation on a series of DNAs. *European Journal of Biochemistry*, 83(2), 375–387. doi:10.1111/j.1432-1033.1978.tb12103.x
- Nafisi, S., Saboury, A. A., Keramat, N., Neault, J.-F., & Tajmir-Riahi, H.-A. (2007). Stability and structural features of DNA intercalation with ethidium bromide, acridine orange and methylene blue. *Journal of Molecular Structure*, 827(1-3), 35–43. doi:10.1016/j.molstruc.2006.05.004
- Neelam, S., Gokara, M., Sudhamalla, B., Amooru, D. G., & Subramanyam, R. (2010). Interaction studies of coumaroyltyramine with human serum albumin and its biological importance. *The Journal of Physical Chemistry B*, 114(8), 3005–3012. doi:10.1021/jp910156k
- Oohara, I., & Wada, A. (1987). Spectroscopic studies on histone–DNA interactions. II. Three transitions in nucleosomes resolved by salt-titration. *Journal of Molecular Biology*, 196(2), 399–411.
- Paul, B. K., & Guchhait, N. (2011). Exploring the strength, mode, dynamics, and kinetics of binding interaction of a cationic biological photosensitizer with DNA: Implication on dissociation of the drug–DNA complex via detergent sequestration. *The Journal of Physical Chemistry B*, 115(41), 11938–11949. doi:10.1021/jp206589e
- Ross, P. D., & Subramanian, S. (1981). Thermodynamics of protein association reactions: Forces contributing to stability. *Biochemistry*, 20(11), 3096–3102. doi:10.1021/bi00514a017
- Sarkar, D., Das, P., Basak, S., & Chattopadhyay, N. (2008). Binding interaction of cationic phenazinium dyes with calf thymus DNA: A comparative study. *The Journal of Physical Chemistry B*, 112(30), 9243–9249. doi:10.1021/jp801659d
- Shahabadi, N., Hadidi, S., & Taherpour, A. A. (2014). Synthesis, characterization, and DNA binding studies of a new Pt (II) complex containing the drug levetiracetam: Combining experimental and computational methods. *Applied Biochemistry and Biotechnology*, 172(5), 2436–2454. doi:10.1007/s12010-013-0695-z
- Shakibapour, N., Dehghani Sani, F., Beigoli, S., Sadeghian, H., & Chamani, J. (2018). Multi-spectroscopic and molecular modeling studies to reveal the interaction between propyl acridone and calf thymus DNA in the presence of histone H1: Binary and ternary approaches. *Journal of Biomolecular Structure and Dynamics*, 1–13. doi:10.1080/07391102.2018.1427629. [Epub ahead of print]
- Sohrabi, T., Hosseinzadeh, M., Beigoli, S., Saberi, M. R., & Chamani, J. (2018). Probing the binding of lomefloxacin to a calf thymus DNA–histone H1 complex by multi-spectroscopic and molecular modeling techniques. *Journal of Molecular Liquids*, 256, 127–138. doi:10.1016/j.molliq.2018.02.031
- Sowrirajan, C., Yousuf, S., & Enoch, I. V. (2014). The unusual fluorescence quenching of Coumarin 314 by β-cyclodextrin and the effect of β-cyclodextrin on its binding with calf thymus DNA. *Australian Journal of Chemistry*, 67(2), 256–265. doi:10.1071/CH13364
- Tang, J., Feng, Y., Tsao, S., Wang, N., Curtain, R., & Wang, Y. (2009). Berberine and Coptidis rhizoma as novel antineoplastic agents: A review of traditional use and biomedical investigations. *Journal of Ethnopharmacology*, 126(1), 5–17. doi:10.1016/j.jep.2009.08.009
- Wang, J., Wang, W., Kollman, P. A., & Case, D. A. (2006). Automatic atom type and bond type perception in molecular mechanical calculations. *Journal of Molecular Graphics and Modelling*, 25(2), 247–260. doi:10.1016/j.jmglm.2005.12.005
- Wang, J., Wolf, R. M., Caldwell, J. W., Kollman, P. A., & Case, D. A. (2004). Development and testing of a general Amber force field. *Journal of Computational Chemistry*, 25(9), 1157–1174.
- Zavriev, S. K., Minchenkova, L. E., Vorlickova, R., & Kolchinsky, A. M., Volkenstein, M. V., & Ivanov, V. I. (1979). Circular dichroism anisotropy of DNA with different modifications at N7 of guanine. *Biochimica et Biophysica Acta*, 564(2), 212–224. doi:10.1016/0005-2787(79)90220-X